Granular Matter (2022) 24:49
https://doi.org/10.1007/s10035-021-01205-3

BRIEF COMMUNICATION

Stress field equations for a disk subjected to self-equilibrated arbitrary loads: revisited

K. Ramesh[1] · **K. Shins**[1]

Received: 29 September 2021 / Accepted: 30 December 2021 / Published online: 17 February 2022

Abstract
Closed-form expressions for stress distribution in a disk subjected to self-equilibrated loads having arbitrary magnitudes and directions have been derived following the approach of Timoshenko. The stress field equations are simplified to a readily usable form by intelligently employing the solution to the problem of a concentrated load acting on a semi-infinite plate (Flamant's solution) and the solution of Lame's problem. The proposed equations eliminate a series of involved and avoidable steps to be followed in the existing methods for stress determination, which makes these new equations computationally more efficient. The isochromatic fringes plotted using the proposed equations for disks subjected to various numbers of loads revealed a subtle aspect that the fringe order at the free boundary of a disk is non-zero if the loads are acting in the non-radial direction whereas it is zero for radial loads. This heuristic information can further simplify the determination of contact forces from isochromatic fringes, which is the current focus of many of the researchers working in the field of granular materials.

Keywords Granular materials · Photoelasticity · Isochromatics

1 Introduction

Photoelasticity has been applied in the study of granular materials for qualitative as well as quantitative analysis of stresses and has picked up momentum in the last decade. In these studies, disks made of polymeric materials that exhibit stress or strain induced birefringence are used as the granular medium. The current research on granular studies are focused on the inverse problem of determination of forces from the photoelastic fringe contours of constant principal stress difference known as isochromatics [1, 2]. The knowledge about the stress state inside a disk subjected to loads of arbitrary magnitudes and directions is essential to achieve this.

In the case of a disk subjected to arbitrary loads, Timoshenko demonstrated that the stresses can be obtained by the superposition of stress components determined using the solution to the problem of a concentrated load acting on a semi-infinite plate and solution to the Lame's problem [3]. Erstwhile researchers have used this approach directly without any further simplifications for the analysis of granular materials to determine the values of contact forces from the isochromatic fringes [2, 4, 5]. A closer look at the equations reveals that multiple mathematical steps involving the determination of stresses with respect to different coordinate systems, transformation of stresses to a common coordinate system and their subsequent addition need to be repeated for each of the loads before determining the stresses due to all the loads for a granule. Since, the number of granules being used is increasing (greater than 10,000), to model the physical phenomenon better, any improvement in the computations can significantly reduce the computational time for analysis.

Surendra and Simha [6] have attempted the solution to the problem of a semi-infinite plate subjected to a concentrated load in a generic case by a sequence of rotation and translation of the reference coordinate axes and appropriate modification of the Airy's stress function. They have reported that the procedure employed gives the solution for the problem of a disk under diametral compression correctly and extended it to find the stress field for three and four arbitrary loads acting on the circular disk. However, they could not present a generalised closed form solution for the problem.

✉ K. Ramesh
kramesh@iitm.ac.in

K. Shins
shinskarthik@gmail.com

[1] Department of Applied Mechanics, Indian Institute of Technology Madras, Chennai 600036, Tamil Nadu, India

In this study, the equations for the stresses in a disk subjected to arbitrary self-equilibrated loads are simplified in terms of the magnitude and direction of loads, and the radius of the disk (R) following the approach of Timoshenko. For completeness, the equations reported by Timoshenko with improved notations of angles along with suitable diagrams are briefly summarised. The proposed equations avoid repeated computations in transforming the stresses from different coordinate systems thereby reducing the computational effort. In view of the simplified equations, an interesting result that can help to identify whether the loads acting on a granule are radial or non-radial is also reported towards the end.

2 Background theory

2.1 Concentrated load acting on a semi-infinite plate (Flamant's problem)

Flamant's solution [7] for the problem of a concentrated load P acting on a semi-infinite plate of thickness h by modifying the 3-dimensional solution by Boussinesq, is the starting point for deriving the stress field equations for a disk, over which self-equilibrated arbitrary boundary loads are acting. If an element is considered at point A as shown in Fig. 1, it will be subjected to a radial stress of magnitude $\sigma_r = \frac{-2P}{\pi h}\frac{\cos\theta^{\mathrm{B}}}{r}$ along the chord BA and $\sigma_\theta = \tau_{r\theta} = 0$ [7], where θ^{B} is the angle between the line of action of the load and the line BA, and r is the distance between the point of application of load and point A.

2.2 Disk subjected to arbitrary loads (solution given by Timoshenko [3])

Now, consider a disk in static equilibrium having thickness h and diameter D subjected to a concentrated load P as shown in Fig. 2. Let A be a point on the boundary of the disk at a distance r from the load application point. The angle between the radial line BO (the line joining the point of application of load and center of the disk) and the line of action of the load measured in the counter-clockwise direction is θ; α is the angle between the radial line BO and positive x-direction; θ_1 and θ_2 are the angles between the line of action of the load and the chords BA and CA, respectively. Using the property of circles, $\angle BAO$ can be found as $\pi/2 - \theta_2$. Let the radial stress acting along the direction of chord BA is σ_r, then, the normal and tangential stresses acting on the boundary of the disk at point A with respect to a polar coordinate system with point O as the origin can be expressed as

$$\sigma_{r_o} = \sigma_r \sin^2\theta_2, \tag{1}$$

$$\tau_{r\theta_o} = -\sigma_r \sin\theta_2 \cos\theta_2. \tag{2}$$

Substituting the value of σ_r from the Flamant's solution and $r = D\sin\theta_2$, Eqs. (1) and (2) can be written as

$$\begin{aligned}\sigma_{r_o} &= \frac{-2P}{\pi hD\sin\theta_2}\cos\theta_1\sin^2\\ \theta_2 &= \frac{-P}{\pi hD}\sin(\theta_1+\theta_2) + \frac{P}{\pi hD}\sin(\theta_1-\theta_2),\end{aligned} \tag{3}$$

$$\begin{aligned}\tau_{r\theta_o} &= \frac{2P}{\pi hD\sin\theta_2}\cos\theta_1\sin\\ \theta_2\cos\theta_2 &= \frac{P}{\pi hD}\cos(\theta_1+\theta_2) + \frac{P}{\pi hD}\cos(\theta_1-\theta_2).\end{aligned} \tag{4}$$

The stresses in Eqs. (3) and (4) can be considered as a superposition of three stresses viz., (i) radial stress of magnitude $\frac{-P}{\pi hD}\sin(\theta_1+\theta_2)$ distributed uniformly on the boundary of the disk, (ii) tangential stress of magnitude $\frac{P}{\pi hD}\cos(\theta_1+\theta_2)$ distributed uniformly on the boundary of the disk, and (iii) stress with normal and tangential components as $\frac{P}{\pi hD}\sin(\theta_1-\theta_2)$ and $\frac{P}{\pi hD}\cos(\theta_1-\theta_2)$, respectively. The angle between the line MM' (parallel to the line of action of force P) and tangent TT' is $\theta_1 - \theta_2$ (Fig. 2), which implies that $\frac{P}{\pi hD}\sin(\theta_1-\theta_2)$ and $\frac{P}{\pi hD}\cos(\theta_1-\theta_2)$ are the components of stress with magnitude $\frac{P}{\pi hD}$ acting in a direction opposite to force P at point A. If 'n' number of loads are acting on a disk in static equilibrium, the stresses that need to be applied at the boundary of the disk to obtain the similar stress distribution are:

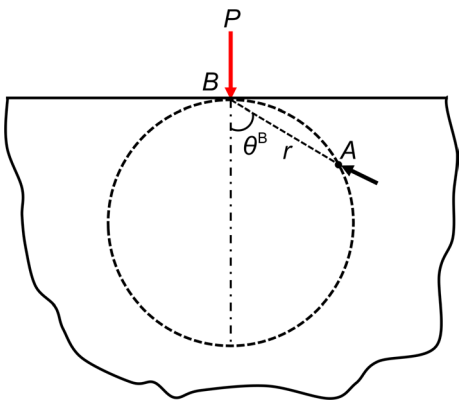

Fig. 1 Concentrated load acting on a semi-infinite plate

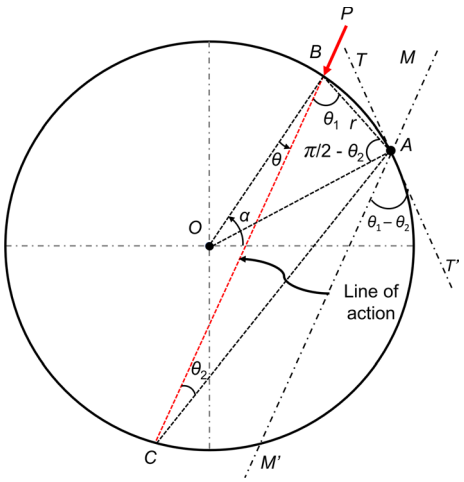

Fig. 2 Arbitrary concentrated load acting on a disk

1. Normal stress of magnitude $\sum_{i=1}^{n} \frac{-P_i}{\pi hD} \sin(\theta_1 + \theta_2)_i = \sum_{i=1}^{n} \frac{-P_i}{\pi hD} \cos\theta_i$ $\left(\because \theta_1 + \theta_2 = \frac{\pi}{2} - \theta\right)$, distributed uniformly on the boundary of the disk.
2. Tangential stress of magnitude $\sum_{i=1}^{n} \frac{P_i}{\pi hD} \cos(\theta_1 + \theta_2)_i$ distributed uniformly on the boundary of the disk. By invoking the torque balance equation for the disk, the sum of the torques with respect to the center of the disk must be zero, i.e., $\sum_{i=1}^{n} \frac{P_i \cos(\theta_1+\theta_2)_i D}{2} = 0$. Therefore, $\sum_{i=1}^{n} \frac{P_i}{\pi hD} \cos(\theta_1 + \theta_2)_i = 0$.
3. Summation of the stresses obtained from the vector sum of $\frac{P_i}{\pi hD} \sin(\theta_1 - \theta_2)_i$ and $\frac{P_i}{\pi hD} \cos(\theta_1 - \theta_2)_i$ which would be zero by invoking the force balance equations for the disk.

The only remaining stress is the radial compressive stress of magnitude $\sum_{i=1}^{n} \frac{-P_i}{\pi hD} \cos\theta_i$. Since the boundary of the disk is stress-free except at the points of application of loads, the effect of this term should be nullified. This can be achieved by applying a uniform radial tension of the same magnitude on the boundary of the disk. Thus, one can express the stress distribution inside a disk subjected to 'n' number of arbitrary loads as the superposition of two stress states:

1. Sum of terms representing the solution for the problem of a concentrated load acting on a semi-infinite plate (Flamant's solution) due to each load,

$$\sigma_r = \sum_{i=1}^{n} \frac{-2P_i}{\pi h} \frac{\cos\theta_i^{\mathrm{B}}}{r_i}. \tag{5}$$

2. Sum of stresses due to radial tension terms introduced for each load,

$$\sigma_{\mathrm{hyd}} = \sum_{i=1}^{n} \frac{P_i}{\pi hD} \cos\theta_i. \tag{6}$$

To illustrate the avoidable repeated computations that are necessary while using the Timoshenko's solution as reported in previous references [2, 4, 5], consider a disk subjected to three radial loads as shown in Fig. 3. For determining the whole field stresses using Timoshenko's solution, the sums of stress terms from the Flamant's solution and radial tension terms have to be determined separately. In Flamant's solution, the stress components are given in polar coordinate system with the point of application of load as the origin and the value of θ^B is measured from the line of action of load. Therefore, for each load, namely, P_1, P_2 and P_3, the origins of the coordinate systems based on which the stresses are

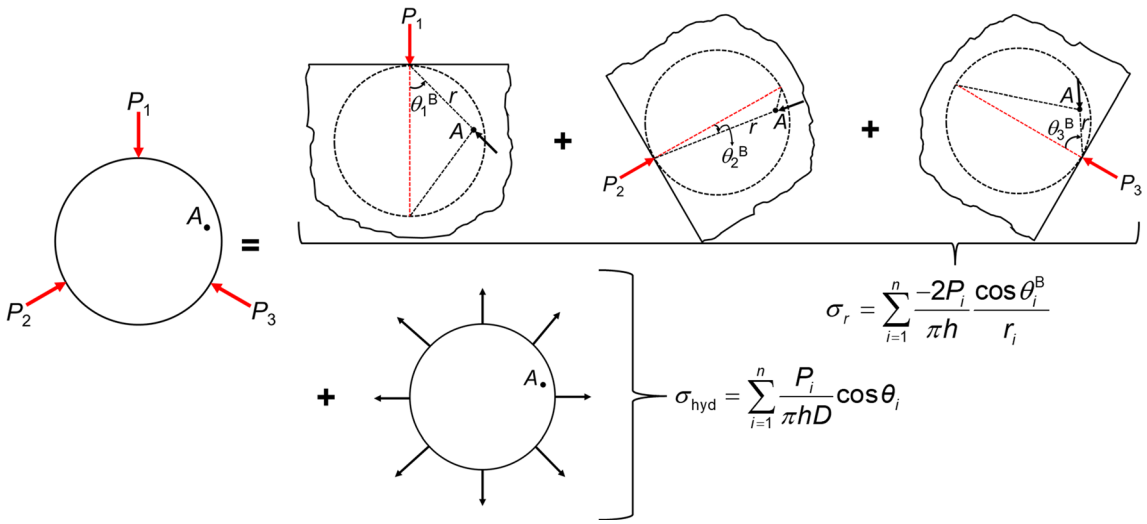

Fig. 3 Demonstration of Timoshenko's solution for the problem of a disk subjected to three radial loads

computed vary. This necessitates suitable coordinate transformations before summing the stress components, making the existing procedure involving repeated avoidable computations.

Even a small improvement is bound to reduce the computational time drastically as very large numbers of granules (exceeding 10,000!) are being used to capture the physical phenomenon of late [8] and the numbers are expected to rise in the future as the field advances further. Therefore, there is a need for simplified closed-form expressions for the stress state in a disk and the simplification is given next.

3 Stress field in Cartesian coordinate system for the disk subjected to arbitrary loads

The components of stresses in Cartesian coordinates for the problem of a disk subjected to arbitrary loads can be obtained by suitably transforming the stress components in Eqs. (5) and (6). Consider a disk of radius R subjected to a concentrated load as shown in Fig. 4. Let the center of the disk be the origin and (x_1, y_1) be the coordinates of the point of application of load. Point A with positional coordinates (x, y) is at a distance r from the point of application of load. The angles α and θ are defined earlier, γ is the angle between the vertical direction and the line joining the point of application of load and the center of the disk, and β is the angle between the vertical direction and the line joining the point of application of load and the point A. The angle θ^{B} is $\beta+\gamma-\theta$, as per the definition. From Fig. 4, it can be shown that $x_1 = R\cos\alpha$, $y_1 = R\sin\alpha$, $\sin\beta = \frac{x-R\cos\alpha}{r}$, $\cos\beta = \frac{R\sin\alpha - y}{r}$, $\sin\gamma = \cos\alpha$, $\cos\gamma = \sin\alpha$, $\cos(\beta+\gamma) = \frac{R-(x\cos\alpha+y\sin\alpha)}{r}$, $\sin(\beta+\gamma) = \frac{x\sin\alpha - y\cos\alpha}{r}$, and $\cos\theta^{\mathrm{B}} = \frac{\left[R-(x\cos\alpha+y\sin\alpha)\right]\cos\theta+(x\sin\alpha-y\cos\alpha)\sin\theta}{r}$.

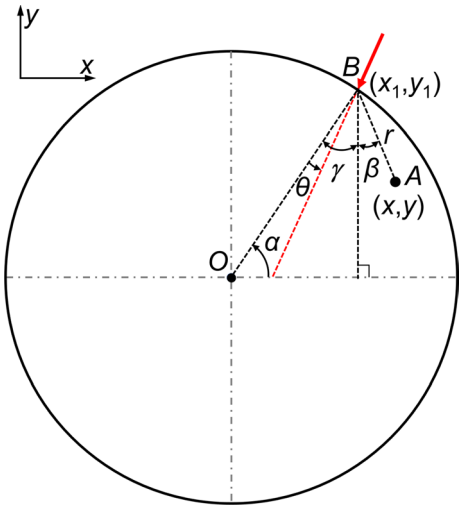

Fig. 4 Definition of angles β and γ

Then, the components of σ_r in the cartesian coordinate system can be obtained as

$$\sigma_x = \frac{-2P}{\pi h}\frac{\cos\theta^{\mathrm{B}}}{r}\sin^2\beta = \frac{-2P}{\pi h}\frac{\left\{\left[R-(x\cos\alpha+y\sin\alpha)\right]\cos\theta+(x\sin\alpha-y\cos\alpha)\sin\theta\right\}(x-R\cos\alpha)^2}{r^4}, \tag{7}$$

$$\sigma_y = \frac{-2P}{\pi h}\frac{\cos\theta^{\mathrm{B}}}{r}\cos^2\beta = \frac{-2P}{\pi h}\frac{\left(\left(R-\left[x\cos\alpha+y\sin\alpha\right]\right)\cos\theta+(x\sin\alpha-y\cos\alpha)\sin\theta\right)(R\sin\alpha-y)^2}{r^4}, \tag{8}$$

and

$$\tau_{xy} = \frac{2P}{\pi h}\frac{\cos\theta^{\mathrm{B}}}{r}\cos\beta\sin\beta = \frac{2P}{\pi h}\frac{\left\{\left[R-(x\cos\alpha+y\sin\alpha)\right]\cos\theta+(x\sin\alpha-y\cos\alpha)\sin\theta\right\}(x-R\cos\alpha)(R\sin\alpha-y)}{r^4}, \tag{9}$$

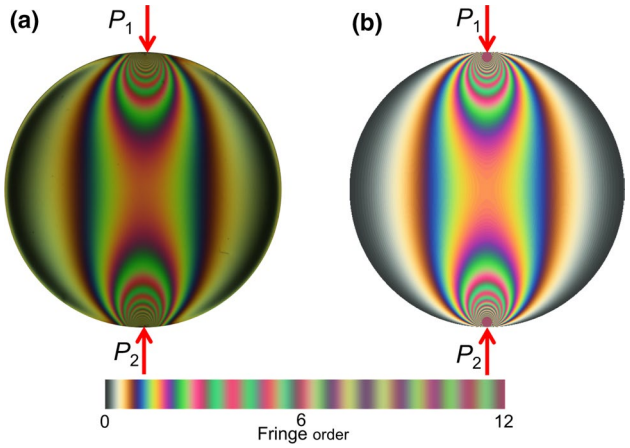

Fig. 5 **a** Isochromatic fringes obtained from the experiment for a disk under diametral compression and **b** the fringes plotted using the proposed equations

where $r = \sqrt{(x-x_1)^2 + (y-y_1)^2}$.

If 'n' number of loads are acting on the disk, the uniform radial tension in Eq. (6) will create a simple hydrostatic state of stress inside the disk with σ_x and σ_y as $\sum_{i=1}^{n} \frac{P_i}{\pi hD} \cos\theta_i$. The final stress distribution can be obtained by adding these terms to the summation of σ_x and σ_y due to each load determined using Eqs. (7) and (8). The closed-form solution for the stresses acting on a disk subjected to loads of arbitrary magnitudes and directions is given as,

$$\sigma_x = \sum_{i=1}^{n} \left(\frac{-2P_i}{\pi h} \frac{\left\{\left[R - \left(x\cos\alpha_i + y\sin\alpha_i\right)\right]\cos\theta_i + \left(x\sin\alpha_i - y\cos\alpha_i\right)\sin\theta_i\right\}\left(x - R\cos\alpha_i\right)^2}{\left((x - R\cos\alpha_i)^2 + (y - R\sin\alpha_i)^2\right)^2} + \frac{P_i}{\pi hD}\cos\theta_i \right), \tag{10}$$

$$\sigma_y = \sum_{i=1}^{n} \left(\frac{-2P_i}{\pi h} \frac{\left\{\left[R - \left(x\cos\alpha_i + y\sin\alpha_i\right)\right]\cos\theta_i + \left(x\sin\alpha_i - y\cos\alpha_i\right)\sin\theta_i\right\}\left(R\sin\alpha_i - y\right)^2}{\left((x - R\cos\alpha_i)^2 + (y - R\sin\alpha_i)^2\right)^2} + \frac{P_i}{\pi hD}\cos\theta_i \right), \tag{11}$$

and

$$\tau_{xy} = \sum_{i=1}^{n} \left(\frac{2P_i}{\pi h} \frac{\left\{\left[R - \left(x\cos\alpha_i + y\sin\alpha_i\right)\right]\cos\theta_i + \left(x\sin\alpha_i - y\cos\alpha_i\right)\sin\theta_i\right\}\left(x - R\cos\alpha_i\right)\left(R\sin\alpha_i - y\right)}{\left((x - R\cos\alpha_i)^2 + (y - R\sin\alpha_i)^2\right)^2} \right). \tag{12}$$

The equations are readily usable and by means of simple substitutions, one can easily obtain the stress field throughout the domain of the disk.

3.1 Solution to the problem of a disk under diametral compression

The stress field expressions for the well-known problem of a disk under diametral compression can be derived by appropriately substituting the values for α and θ in Eqs. (10)–(12). Consider a disk subjected to diametral compression, as shown in Fig. 5. Let P be the magnitude of each load ($P_1 = P_2 = P$), the values of α for P_1 and P_2 are 90° and –90°, respectively and the value of θ is zero for both the loads. Substituting these values in the proposed stress field equations, the stress components are obtained as

$$\begin{Bmatrix} \sigma_x \\ \sigma_y \\ \tau_{xy} \end{Bmatrix} = -\frac{2P}{\pi h} \begin{Bmatrix} \frac{(R-y)\,x^2}{r_1^4} + \frac{(R+y)\,x^2}{r_2^4} - \frac{1}{D} \\ \frac{(R-y)^3}{r_1^4} + \frac{(R+y)^3}{r_2^4} - \frac{1}{D} \\ \frac{(R+y)^2 x}{r_2^4} - \frac{(R-y)^2 x}{r_1^4} \end{Bmatrix}, \tag{13}$$

where, $r_1 = \sqrt{x^2 + (R-y)^2}$ and $r_2 = \sqrt{x^2 + (R+y)^2}$. Equation (13) is the standard solution for the problem of the disk under diametral compression [7, 9].

3.2 Isochromatic fringes on a disk subjected to arbitrary loads

The usefulness of the proposed equations [Eqs. (10)–(12)] can be demonstrated by theoretically plotting the isochromatic fringes. In photoelasticity experiments, colour isochromatic fringes are obtained when white light is used while black and white fringes are obtained when monochromatic light is used. Fringe order throughout the domain of the disk

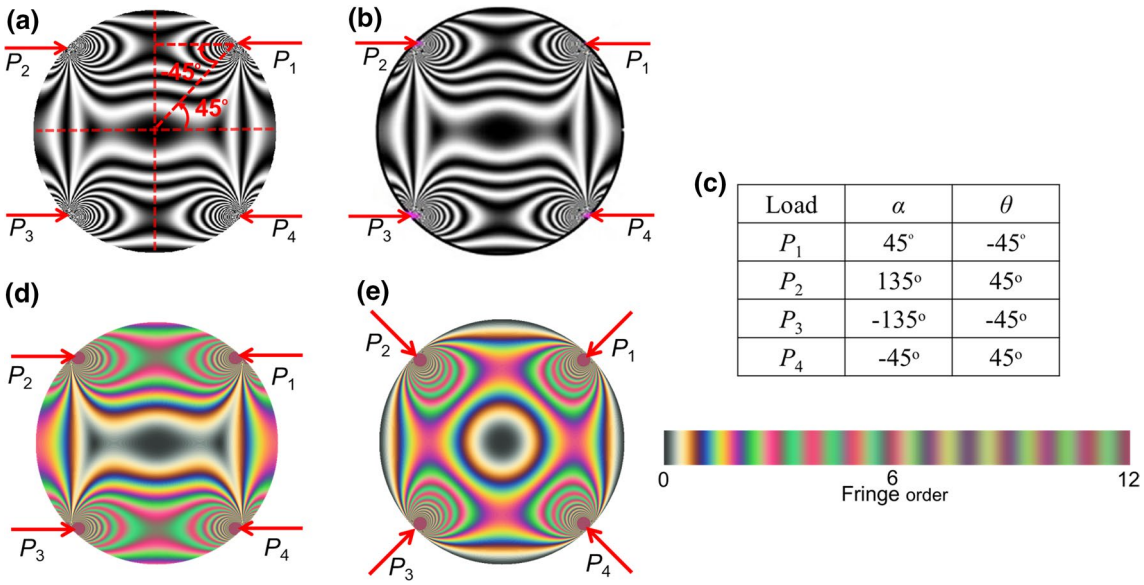

Fig. 6 Isochromatic fringes plotted for four non-radial loads acting on a disk **a** using the proposed equations, **b** from Ref. [11] using the same photoelastic and material parameters and **c** values of α and θ corresponding to image 'a'. **d** Isochromatic fringes corresponding to image 'a' plotted in colour and **e** isochromatic fringes if the loads are acting in the radial direction

is calculated from the principal stress difference by invoking the stress-optic law [9]. Then, the exit light intensity is determined from the fringe orders and plotted [9]. To obtain the colour isochromatics, first, an experimental calibration table in the range of 0–12 fringe orders containing the greyscale values for the three image planes R, G, and B corresponding to the fringe orders are obtained. Subsequently, the fringe orders in the disk are matched with the calibration table and the RGB values are correspondingly allotted to get the isochromatics in colour [10].

The experimental dark field isochromatic fringes for a disk of diameter 60 mm under diametral compression with a load of 492 N is shown in Fig. 5a. The simulated isochromatics using the proposed equations are shown in Fig. 5b that compare well with the Fig. 5a. The isochromatic fringes are also plotted for the case of four non-radial loads acting on a disk using the parameters used by Zhao et al. [11] (Fig. 6a). The method to determine the values of α and θ for load P_1 is also shown in Fig. 6a. Figure 6b shows the fringes obtained by Zhao et al., which compares well with Fig. 6a. The values of α and θ for loads P_1 to P_4 are summarized in Fig. 6c. It is desirable to plot the fringes in colour as one can determine the fringe order using the colour code. A black colour indicates that the fringe order is zero. Figure 6d shows the isochromatics plotted in colour and one can observe that on the free outer boundary of the disk, the colour varies depending on the location. Figure 6e shows the isochromatics plotted for the case when the external loads are radial at these points. The free outer boundary is uniformly black indicating zeroth fringe order. Same is the case for the disk under diametral compression (Fig. 5b), where again the loads are radial.

The isochromatic fringes plotted in colour brings out a subtle aspect that if the loads are acting in the radial direction on the boundary of the disk, the fringe order observed on the free boundary would be zero. But, if the loads are non-radial, the fringe order at the free boundary is not zero. This is due to the fact that when the contact loads are not radial, the free outer boundary can sustain $\sigma_{\theta\theta}$ still maintaining the outer surface as free! This can be appreciated from Fig. 7 which shows the variation of stress components in polar and Cartesian coordinate system along the boundary of

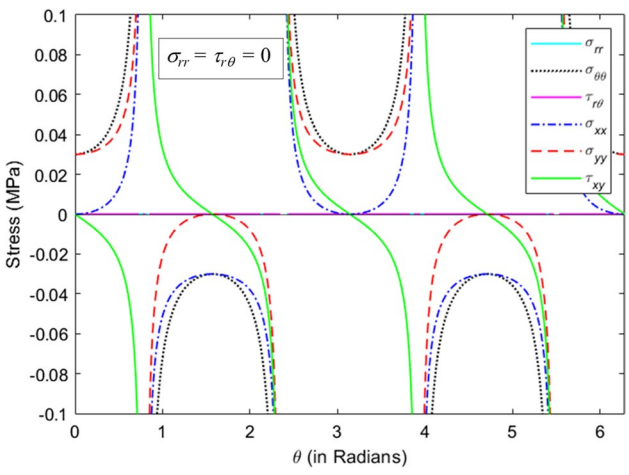

Fig. 7 Variation of stresses for a disk subjected to four non-radial loads as shown in Fig. 6a

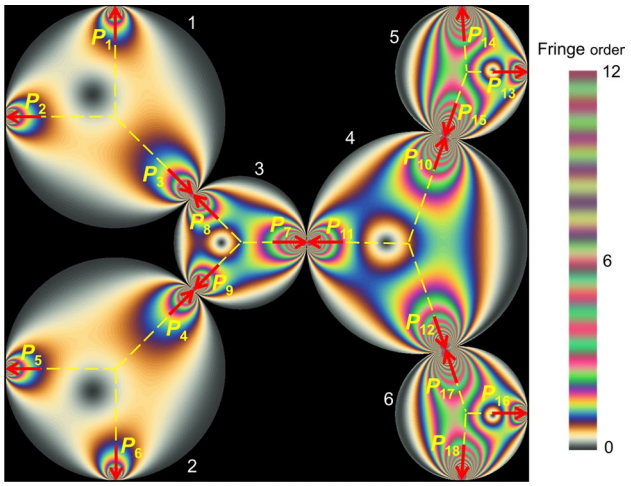

Fig. 8 Force chain in a granular system plotted using the proposed equations

Table 1 Magnitude, α, and θ corresponding to each load in Fig. 8

Load	Magnitude (N)	α (°)	θ (°)
P_1	20	90	0
P_2	20	180	0
P_3	28.28	− 45	0
P_4	28.28	45	0
P_5	20	180	0
P_6	20	− 90	0
P_7	40	0	0
P_8	28.28	135	0
P_9	28.28	− 135	0
P_{10}	61.43	75	− 4
P_{11}	40	180	0
P_{12}	61.43	− 75	4
P_{13}	24.28	0	0
P_{14}	58.24	90	4.22
P_{15}	61.43	− 105	− 4
P_{16}	24.28	0	0
P_{17}	61.43	105	4
P_{18}	58.24	− 90	− 4.22

the disk shown in Fig. 6a. The thickness of the disk is taken as 6 mm. It is evident that the value of $\sigma_{\theta\theta}$ is not zero consequently making the components of stresses in Cartesian coordinate system obtained by stress transformation also as non-zero. In the case of radial loads as shown in Fig. 6e, $\sigma_{\theta\theta}$ will also be zero in turn making all the other stress components as zero.

This aspect will be helpful in identifying the radial/non-radial loads directly in the analysis of granular materials if coloured isochromatics are used in the analysis. In the inverse analysis of granular materials for the determination of contact forces from the isochromatic fringes, if the disks subjected to only radial loads can be identified prior to the analysis, it will considerably reduce the number of unknowns involved in the problem which further reduces the computational effort required thereby improving efficiency.

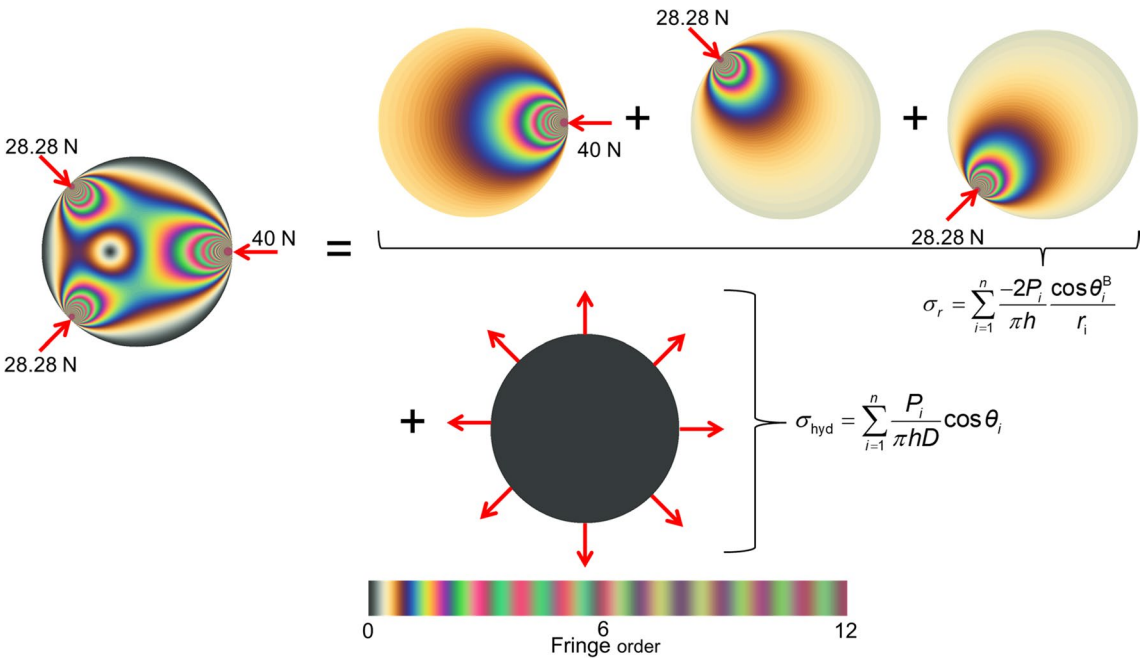

Fig. 9 Isochromatic fringes showing the superposition of stresses in disk number 3 in Fig. 8

3.3 Force chains in granular materials

The proposed stress field equations have significant application in the area of granular materials research. In granular systems, the distribution of forces is not homogeneous, and it occurs through various pathways connecting the granular particles termed as *force chains* [12, 13]. Figure 8 shows the representation of a force chain plotted in the dark field arrangement of the polariscope using the proposed stress field equations. The material stress fringe value used is 8 N/mm/fringe, and the diameters of large and small disks are 10 and 6 mm, respectively. Here, the forces acting on the disks are in the radial direction for most of the cases and hence the value of θ is zero; the forces P_{10}, P_{12}, P_{14}, P_{15}, P_{17} and P_{18} are exceptions. The complete details of the magnitudes and directions of the forces acting on each disk is given in Table 1. To visually appreciate the superposition of stresses, the isochromatic fringes for disk number 3 in Fig. 8 is provided in Fig. 9.

4 Conclusion

In this study, the generic equations that are readily usable to find the stress field inside a disk subjected to self-equilibrated loads of arbitrary magnitudes and directions are derived. The usefulness of the equations is demonstrated by theoretically plotting the isochromatic fringes for various numbers of self-equilibrated loads and compared with experimentally obtained fringes.

The current set of simplified equations have helped to ascertain how one can identify existence of non-radial loads on the boundary by using the colour information of isochromatic fringes obtained through photoelasticity. The force solvers can now use the heuristic information on whether the forces acting in a particular granule are radial or non-radial by monitoring the fringe data on the boundary of the disk—thereby potentially reducing the computational time. This information can also be useful in machine learning algorithms used in the analysis of granular materials.

Funding The authors did not receive support from any organization for the submitted work.

Declarations

Conflict of interest The authors have no conflicts of interest to declare that are relevant to the content of this article.

References

1. Sergazinov, R., Kramar, M.: Machine learning approach to force reconstruction in photoelastic materials, pp. 1–20 (2020) [Online]. http://arxiv.org/abs/2010.01163
2. Daniels, K.E., Kollmer, J.E., Puckett, J.G.: Photoelastic force measurements in granular materials. Rev. Sci. Instrum. **88**(5), 051808 (2017). https://doi.org/10.1063/1.4983049
3. Timoshenko, S., Goodier, J.N.: Theory of elasticity. McGraw Hill Education (1951)
4. Majmudar, T.S.: Experimental studies of two-dimensional granular systems using grain-scale contact force measurements. Graduate School of Duke University (2006)
5. Puckett, J.G.: State variables in granular materials: an investigation of volume and stress fluctuations. North Carolina State University (2012)
6. Surendra, K.V.N., Simha, K.R.Y.: Characterizing frictional contact loading via isochromatics. Exp. Mech. **54**(6), 1011–1030 (2014). https://doi.org/10.1007/s11340-014-9865-3
7. Martin, H.S.: Elasticity-Theory, Applications and Numerics. Elsevier (2005)
8. Daniels, K.E., Hayman, N.W.: Force chains in seismogenic faults visualized with photoelastic granular shear experiments. J. Geophys. Res. **113**(B11), B11411 (2008). https://doi.org/10.1029/2008JB005781
9. Ramesh, K.: Digital Photoelasticity Advanced Techniques and Applications. Springer, Berlin, Heidelberg (2000). https://doi.org/10.1115/1.1483353
10. Ramesh, K.: Developments in Photoelasticity—A Renaissance. IOP Publishing (2021). https://doi.org/10.1088/978-0-7503-2472-4
11. Zhao, Y., Zheng, H., Wang, D., Wang, M., Behringer, R.P.: Particle scale force sensor based on intensity gradient method in granular photoelastic experiments. New J. Phys. **21**(2), 023009 (2019). https://doi.org/10.1088/1367-2630/ab05e7
12. Abed Zadeh, A., et al.: Enlightening force chains: a review of photoelasticimetry in granular matter. Granul. Matter **21**(4), 1–12 (2019). https://doi.org/10.1007/s10035-019-0942-2
13. Abed-Zadeh, A., Barés, J., Brzinski, T., Daniels, K.E., Dijksman, J., Docquier, N., Everitt, H., Kollmer, J., Lantsoght, O., Wang, D., Workamp, M., Zhao, Y., Zheng. Home · Wiki · PhotoElasticity_Main · GitLab